Published in final edited form as:
Neuron. 2010 December 22; 68(6): 1143–1158. doi:10.1016/j.neuron.2010.11.034.

Local presynaptic activity gates homeostatic changes in presynaptic function driven by dendritic BDNF synthesis

Sonya K. Jakawich[1,2], **Hassan B. Nasser**[2], **Michael J. Strong**[2], **Amber J. McCartney**[1,2], **Amanda S. Perez**[2], **Neal Rakesh**[2], **Cynthia J. L. Carruthers**[2], and **Michael A. Sutton**[1,2,*]

[1] Neuroscience Graduate Program, and Department of Molecular and Integrative Physiology, University of Michigan, Ann Arbor, MI 48109

[2] Molecular and Behavioral Neuroscience Institute, and Department of Molecular and Integrative Physiology, University of Michigan, Ann Arbor, MI 48109

SUMMARY

Homeostatic synaptic plasticity is important for maintaining stability of neuronal function, but heterogeneous expression mechanisms suggest that distinct facets of neuronal activity may shape the manner in which compensatory synaptic changes are implemented. Here, we demonstrate that local presynaptic activity gates a retrograde form of homeostatic plasticity induced by blockade of AMPA receptors (AMPARs) in cultured hippocampal neurons. We show that AMPAR blockade produces rapid (< 3 hrs) protein synthesis-dependent increases in both presynaptic and postsynaptic function, and that the induction of presynaptic, but not postsynaptic, changes requires coincident local activity in presynaptic terminals. This “state-dependent” modulation of presynaptic function requires postsynaptic release of brain-derived neurotrophic factor (BDNF) as a retrograde messenger, which is locally synthesized in dendrites in response to AMPAR blockade. Taken together, our results reveal a local cross-talk between active presynaptic terminals and postsynaptic signaling that dictates the manner by which homeostatic plasticity is implemented at synapses.

Keywords

homeostatic plasticity; retrograde signaling; BDNF; local protein synthesis; miniature neurotransmission

INTRODUCTION

Activity-dependent forms of synaptic plasticity such as long-term potentiation (LTP) and long-term depression (LTD) have long been considered primary candidates for cellular mechanisms of information storage, but only over the last decade has there been wide interest in understanding how neural circuits maintain stability by offsetting the destabilizing nature of these synaptic modifications. It is now known that central neurons have the potential to adapt to changing activity levels by invoking compensatory changes in synaptic

*to whom correspondence should be addressed: Michael A. Sutton, Molecular and Behavioral Neuroscience Institute, 5067 BSRB, 109 Zina Pitcher Place, University of Michigan, Ann Arbor, MI 48109-2200; 734-615-2445 (phone), 734-936-2690 (fax); masutton@umich.edu.

function (Davis, 2006; Turrigiano, 2008; Pozo and Goda, 2010). In central neurons, such homeostatic forms of synaptic plasticity are typically studied in the context of chronic perturbations of neural activity in networks of cultured neurons, where persistent activity elevation or suppression is met with a gradual weakening or strengthening of synaptic efficacy, respectively (Turrigiano et al., 1998; O'Brien et al., 1998).

Recent studies have revealed that homeostatic synaptic plasticity is associated with heterogeneous expression mechanisms. During activity deprivation, homeostatic changes at excitatory synapses can manifest as an increase in postsynaptic sensitivity to glutamate (Turrigiano et al., 1998; O'Brien et al., 1998; Wierenga et al., 2005; Sutton et al., 2006), an increase in presynaptic neurotransmitter release (Murthy et al., 2001; Burrone et al., 2002), or some combination of the two (Thiagarajan et al., 2005; Gong et al., 2007). While cell type or developmental age (Wierenga et al., 2006; Echegoyen et al., 2007) may contribute to these differences, recent evidence suggests that the same synapse can exhibit different forms of synaptic compensation tuned to distinct facets of neural activity. Chronic action potential (AP) blockade with tetrodotoxin (TTX) typically induces a slow (> 12 hrs) scaling of postsynaptic function (Turrigiano et al., 1998; Sutton et al., 2006), that is associated with a synaptic accumulation of AMPA-type glutamate receptors (AMPARs) that contain the GluA2 subunit (Wierenga et al., 2005; Sutton et al., 2006; Ibata et al., 2008). By contrast, coincident blockade of APs and miniature synaptic events induces a greatly accelerated homeostatic increase in postsynaptic function (Sutton et al., 2006) mediated by *de novo* dendritic synthesis of GluA1 and the incorporation of GluA2-lacking AMPARs at synapses (Sutton et al., 2006; Aoto et al., 2008; see also, Ju et al., 2004). Chronic (24 hr) AMPAR blockade (without coincident AP blockade) also induces postsynaptic compensation that requires synaptic incorporation of GluA2-lacking AMPARs, but importantly, an increase in presynaptic release probability is also observed (Thiagarajan et al., 2005; Gong et al., 2007). Furthermore, at the *Drosophila* neuromuscular junction, Frank et al. (2006) also observed a rapid homeostatic adjustment of synaptic efficacy when miniature events were blocked, but these changes were observed in quantal content and were thus reflective of a presynaptic expression mechanism. Hence, while there is convergent support for the role of miniature synaptic events in homeostatic synaptic plasticity, it is still unclear why direct blockade of excitatory postsynaptic drive can recruit corresponding presynaptic changes in some circumstances, but not others.

A defining feature of synapses in the neocortex and hippocampus is a tight correspondence of pre- and post-synaptic structure indicative of strong functional matching on either side of the synapse. Given that many forms of both homeostatic and Hebbian synaptic plasticity are initially mediated by functional changes that are restricted to the postsynaptic compartment, there must be some mechanism that can recruit corresponding changes in presynaptic function in a retrograde fashion. Indeed, a number of studies have documented such retrograde influences on presynaptic structure and function induced by chronic manipulations of postsynaptic activity and/or function (e.g., Paradis et al., 2001; Pratt et al., 2003; Branco et al., 2008). These observations thus raise the question of whether homeostatic adjustment of synapse function is influenced not only by the severity of activity deprivation, but also by the extent to which neurons retain certain activity-dependent signaling capabilities.

Here, we identify a retrograde signaling mechanism in hippocampal neurons that coordinates homeostatic changes in pre- and postsynaptic function. We show that blocking excitatory synaptic drive through AMPARs not only produces faster postsynaptic compensation compared with AP blockade, it also induces retrograde enhancement of presynaptic function that is prevented by coincident AP blockade. This sensitivity to AP blockade reflects state-dependent gating of these presynaptic changes by local activity in

presynaptic terminals. Finally, we demonstrate that the local cross-talk between postsynaptic activity and presynaptic function is mediated by local dendritic release of BDNF as a retrograde messenger, which is required downstream of protein synthesis for the presynaptic changes induced by AMPAR blockade. Our results thus demonstrate a link between local control of protein synthesis in dendrites and activity-dependent transynaptic modulation of presynaptic function.

RESULTS

AMPAR blockade induces state-dependent changes in presynaptic function

We first compared the homeostatic regulation of synapse function induced by chronic (24 hr) AP blockade (2 μM TTX), chronic AMPAR blockade (10 μM NBQX), or a combination of the two (NBQX+TTX). Both AP and AMPAR blockade profoundly decrease excitatory synaptic drive, but each spares a distinct facet of neuronal activity: AP blockade spares miniature neurotransmission, whereas AMPAR blockade spares the capacity for neurons to spontaneously fire APs (confirmed by loose-patch recordings; data not shown). Consistent with previous studies, we found that chronic AP blockade produced a significant increase in mEPSC amplitude, without a corresponding change in mEPSC frequency (Figure 1A–C). Likewise, chronic AMPAR blockade produced a significant increase in mEPSC amplitude, revealed upon NBQX washout, but also a significant increase in mEPSC frequency as reported by others (Murthy et al., 2001; Thiagarajan et al., 2005; Gong et al., 2007). Interestingly, when co-applied over 24 hrs, TTX specifically prevented the increase in mEPSC frequency induced by NBQX, without affecting the increase in mEPSC amplitude (Figure 1A–C). While coincident TTX application prevented the induction of NBQX-dependent changes in mEPSC frequency, it did not prevent the expression of these changes - the increase in mEPSC frequency induced by NBQX alone persisted for at least 60 min with continuous presence of TTX in the recording ringer. These results suggest that chronic AP blockade is effective in establishing compensatory postsynaptic changes, it also appears to specifically prevent the development of compensatory presynaptic changes.

As previous studies have demonstrated rapid forms of homeostatic plasticity induced by direct blockade of synaptic activity (Sutton et al., 2006; Frank et al., 2006), we next asked whether the changes in mEPSC amplitude or frequency that accompany AMPAR blockade develop with different kinetics than the scaling of mEPSC amplitude induced by AP blockade alone. Confirming previous observations (Turrigiano et al., 1998; Sutton et al., 2006), we found that a relatively brief period of AP blockade (2 μM TTX, 3 hrs) was insufficient to alter mEPSC frequency or amplitude (Figure 1D–F). However, brief periods of AMPAR blockade (40 μM CNQX, 3 hrs) induced significant increases in both mEPSC amplitude and frequency (Figure 1D–F), consistent with an increase in both pre- and post-synaptic function. Again, we found that coincident AP blockade during induction (TTX +CNQX, 3 hrs) specifically prevented the increase in mEPSC frequency without altering the scaling of mEPSC amplitude induced by brief AMPAR blockade (Figure 1D–F). These results suggest that AMPAR blockade recruits a “state-dependent” increase in presynaptic release probability – the induction of these presynaptic changes requires that neurons retain the capacity for AP firing.

The state-dependent increase in mEPSC frequency observed after AMPAR blockade could reflect a persistent increase in presynaptic function. Alternatively, it could reflect a postsynaptic unsilencing of AMPAR lacking synapses, since enhanced AMPAR expression at synapses is associated with homeostatic increases in synapse function (O’Brien et al., 1998; Wierenga et al., 2005; Thiagarajan et al., 2005; Sutton et al., 2006). However, we found that AMPAR blockade enhances surface expression of the AMPAR subunit GluA1 at PSD95-labeled excitatory synapses to a similar extent regardless of whether spiking was

permitted or prevented with coincident TTX application (Figure 1G–H and Figure S1). To monitor changes in presynaptic function directly, we examined the activity-dependent uptake of an antibody against the lumenal domain of synaptotagmin 1 (syt-lum) at excitatory synapses marked by immunoreactivity for the vesicular glutamate transporter (vglut1). Syt-lum uptake is still visible under stringent permeabilization conditions necessary to efficiently co-label synaptic sites in the same cells, and thus provides a direct measure of presynaptic function where overall synaptic density is internally controlled. We first validated the activity-dependent nature of syt-lum uptake at synaptic sites using direct depolarization of synaptic terminals (60 mM K^+), and confirmed that the AP-independent uptake of syt-lum is synaptic (Figure S2). We then assessed excitatory presynaptic function after 3 hr AMPAR blockade using synaptic syt-lum uptake as a read-out. Prior to labeling, neurons were exposed to 2 μM TTX for 15 min to isolate spontaneous neurotransmitter release. As a measure of presynaptic function, we quantified the percentage of vglut1-positive excitatory synaptic terminals with accompanying syt-lum staining. We found that 3 hr AMPAR blockade enhanced presynaptic function relative to untreated controls and neurons experiencing a blockade of APs alone with TTX (Figure 1I,J and Figure S3). Moreover, coincident blockade of both AMPARs and spiking prevented the increase in syt-lum uptake, similar to the state-dependent enhancement of mEPSC frequency revealed by electrophysiology. A similar pattern of results was observed using presynaptic FM4-64X labeling (Figure S3). These effects on presynaptic function were not associated with a change in overall density of excitatory synapses (Figure S3), illustrating that AMPAR blockade regulates the function of existing excitatory synaptic terminals.

While AMPAR blockade removes excitatory synaptic drive, it does not prevent neurons from spiking spontaneously (data not shown), raising the possibility that state-dependent changes in presynaptic function require presynaptic spiking. To test this possibility, we used a cocktail of 1 μM ω-conotoxin GVIA and 200 nM ω-agatoxin IVA; CTx/ATx), to block P/Q and N-type $Ca2^+$ channels that are localized to presynaptic terminals and normally support AP-mediated neurotransmission (Wheeler et al., 1994). We found that, like TTX treatment, coincident P/Q/N-type $Ca2^+$ channel blockade completely prevented the increase in synaptic syt-lum uptake induced by 3 hr AMPAR blockade (Figure 1J). In a parallel set of experiments, we similarly found that coincident CTx/ATx treatment specifically prevented the increase in mEPSC frequency induced by AMPAR blockade (Mean ± SEM mEPSC frequency, control = 1.43 ± 0.26 Hz; 3hr CNQX = 3.37 ± 0.58 Hz, $p < 0.05$; CNQX + CTx/ATx = 1.15 ± 0.11 Hz, NS; n = 12, 10, 10; data not shown). Finally, we also examined whether the changes in presynaptic function reflected by spontaneous synaptic vesicle exocytosis extended to changes in evoked release by washing out CNQX (or CNQX+TTX) after 3 hrs and measuring paired-pulse facilitation (PPF). As expected for an increase in evoked release probability, we found that AMPAR blockade significantly inhibited PPF whereas coincident TTX application with CNQX fully restored PPF to control levels (Figure 1K–L). Together, these results demonstrate that AMPAR blockade induces two qualitatively distinct compensatory changes at synapses: an increase in postsynaptic function that is induced regardless of spiking activity, and a state-dependent enhancement of presynaptic function that requires coincident presynaptic activity.

NMDAR blockade induces rapid postsynaptic, but not presynaptic, compensation

We next asked whether the homeostatic changes in presynaptic function are driven by AMPAR blockade specifically, or whether they are also evident following NMDAR blockade. We first addressed this issue using mEPSC recordings following 3 hr AMPAR blockade (10 μM NBQX) or 3 hr NMDAR blockade (50 μM APV). We found that whereas both AMPAR and NMDAR blockade induced rapid postsynaptic compensation reflected as an increase in mEPSC amplitude, significant changes in mEPSC frequency emerged after

blockade of AMPARs, but not NMDARs (Figure S4). Similarly, 3 hr NBQX treatment significantly enhanced syt-lum uptake at synapses, whereas APV treatment did not (Figure S4). Since rapid postsynaptic compensation induced by NMDAR blockade is mediated by the synaptic recruitment of GluA1 homomeric receptors (Sutton et al., 2006; Aoto et al., 2008), we also examined the functional role of GluA1 homomers after brief (3 hr) AMPAR blockade. We found that following 3 hr CNQX treatment, addition of 1-Napthylacetylspermine (Naspm; a polyamine toxin that specifically blocks AMPARs that lack the GluA2 subunit) during recording reverses the increase in mEPSC amplitude back to control levels, while having no effect in control neurons (Figure S5). Interestingly, while Naspm also decreased mEPSC frequency in a subset of neurons recorded following AMPAR blockade, mEPSC frequency in the presence of Naspm remained significantly elevated relative to control neurons (Figure S5). The differential sensitivity of mEPSC frequency and amplitude to both NMDAR blockade and Naspm suggests that the presynaptic and postsynaptic changes are induced in parallel and are at least partially independent. These results suggest that whereas similar postsynaptic adaptations accompany blockade of AMPARs or NMDARs, the compensatory presynaptic changes are uniquely sensitive to AMPAR activity.

Local activity at presynaptic terminals is required for retrograde modulation of presynaptic function

Does the requirement for either spiking or voltage-gated Ca2+ channels reflect a global network/cell-wide effect or does local activity at presynaptic terminals gate such changes? To distinguish between these possibilities, we examined syt-lum uptake after local microperfusion of either TTX or P/Q/N-type $Ca2^{+}$ channel blockers coupled with global AMPAR blockade (bath application of 20 μM CNQX). Local perfusion was initiated, and 5 min later, CNQX was bath applied for 2 hrs (total local perfusion time of 125 min). Cells were then treated with 2 μM TTX, live-labeled with syt-lum, fixed, and processed for immunostaining against vglut1. As before, we assessed presynaptic function by quantifying the proportion of vglut1-positive excitatory synapses that were also labeled with syt-lum. While local perfusion of vehicle during global AMPAR blockade did not affect the increase in syt-lum uptake, local administration of either TTX or CTx/ATx produced a significant decrease in presynaptic syt uptake in the perfused area relative to apposed terminals on neighboring sections of the same dendrite (Figure 2). As an internal control, no differences were observed in vglut1 density (Figure 2C) or vglut 1 particle intensity (data not shown) in the perfused area relative to terminals on apposing dendritic segments outside of the perfusion area. The local decrease in presynaptic release probability induced by CTx/ATx required coincident AMPAR blockade, since no changes in syt-lum uptake were observed in the treated area when bath CNQX was omitted (Figure 2D); similar results were found in control experiments using local TTX treatment in the absence of CNQX (Bath Vehicle + local TTX, Mean ± SEM proportion of vglut particles with syt-lum, Untreated areas = 0.31 ± 0.04; Treated area = 0.33 ± 0.06, NS, n = 5 dendrites, 3 neurons). Taken together, these data indicate that AMPAR blockade induces retrograde enhancement of presynaptic function that is gated by local activity in presynaptic terminals.

Postsynaptic BDNF release is required for compensatory presynaptic, but not postsynaptic changes

How does postsynaptic activity blockade lead to sustained increases in presynaptic function? Acute BDNF application can rapidly drive increases in presynaptic function (e.g., Alder et al., 2005; Zhang and Poo, 2002), and extended BDNF exposure can induce structural changes at presynaptic terminals (e.g., Tyler and Pozzo-Miller, 2001) suggestive of sustained changes in presynaptic release that may persist when BDNF is no longer present. Consistent with the notion that endogenous BDNF is required for the sustained changes in

presynaptic function induced by AMPAR blockade, we found that scavenging endogenous extracellular BDNF (with TrkB-Fc; 1 μg/ml) or blocking downstream receptor tyrosine kinase signaling (with the Trk inhibitor k252a; 100 nM) during AMPAR blockade both specifically block the increase in syt-lum uptake (Figure 3A–B), but do not produce changes in overall synapse density (Figure S6). Importantly, neither TrkB-Fc nor k252a affected syt-lum uptake in neurons when CNQX and TTX are co-applied, indicating that these effects are specific for the state-dependent changes in presynaptic function. Interestingly, sequestering BDNF did not affect the enhancement of surface GluA1 expression at synaptic sites during AMPAR blockade (Figure 3C–D). Similarly, we found that co-application of TrkB-Fc with CNQX completely prevents the state-dependent increase in mEPSC frequency induced by AMPAR blockade, but does not reduce the increase in mEPSC amplitude (Figure 3E–G), suggesting that endogenous BDNF-driven signaling appears to play a specific role in presynaptic compensation. To confirm that postsynaptic BDNF is necessary for the enhancement of presynaptic function induced by AMPAR blockade, we transfected neurons with shRNAs against BDNF or a scrambled control shRNA; transfected neurons were identified by RFP expression, expressed from an independent promoter in each shRNA plasmid. Two distinct BDNF shRNAs effectively knocked-down BDNF expression relative to the scrambled control, as revealed by BDNF immunocytochemistry 24 hrs post-transfection (Figure 3H–J). The low transfection efficiency (< 1% of neurons) allowed us to examine selective loss of BDNF from a postsynaptic neuron surrounded by untransfected neurons that are otherwise unpeturbed. Hence, mEPSC recordings from transfected neurons revealed that postsynaptic BDNF knockdown (21 hrs prior to AMPAR blockade) did not alter the enhancement of mEPSC amplitude but selectively blocked the increase in mEPSC frequency following brief periods of AMPAR blockade (3 hr CNQX, Figure 3K–M). Taken together, these results suggest that BDNF release from the postsynaptic neuron is essential for homeostatic retrograde enhancement of presynaptic function.

BDNF is sufficient to drive state-dependent changes in presynaptic function

We next examined whether BDNF exposure was sufficient to mimic state-dependent enhancement of presynaptic function observed after AMPAR blockade. We treated neurons with varying durations and concentrations of human recombinant BDNF, then washed off BDNF and assayed spontaneous syt-lum uptake. We found that direct BDNF application induces sustained changes in presynaptic function in a time- and concentration-dependent manner, while co-application of TTX or CTx/ATx with BDNF completely prevents this effect (Figure 4A–C). These changes in function were not associated with overall changes in synapse density (Figure S6), suggesting that like AMPAR blockade, BDNF enhances the function of existing presynaptic terminals. By contrast, BDNF application had no significant effect on surface GluA1 expression at synapses (Figure S6), suggesting a selective presynaptic role. Additionally, we found that BDNF application (250ng/ml, 10 min) enhanced mEPSC frequency within minutes, but these changes rapidly reversed upon BDNF washout (data not shown). By contrast, longer exposure to BDNF (250 ng/ml, 2 hrs) induced a robust and sustained increase in mEPSC frequency, which was prevented by AP or P/Q/N-type Ca2+ channel blockade coincident with BDNF exposure (Figure 4D,E). Since both AMPAR blockade and BDNF treatment induce sustained increases in mEPSC frequency, we next examined whether these effects were additive. Treating neurons with BDNF for the last 2 hrs of AMPAR blockade produced no greater increase in mEPSC frequency than observed in either condition alone (Figure 4F,G), demonstrating that the sustained increase in presynaptic function induced by CNQX treatment occludes such enhancement induced by direct BDNF application. Finally, to examine whether this role of BDNF is local or more global, we locally scavenged BDNF (via restricted perfusion of TrkB-Fc) during AMPAR blockade (120 min CNQX) and found that the increase in syt-lum uptake was disrupted at presynaptic terminals in the treated area; in the absence of AMPAR blockade (Bath vehicle),

local TrkB-Fc had no effect (Figure S7). Conversely, direct local application of BDNF (250 ng/ml, 60 min) induced a selective increase in syt-lum uptake at terminals in the treated area, relative to untreated terminals terminating on the same dendrite (Figure S7). Taken together, these results suggest a model whereby AMPAR blockade triggers dendritic BDNF release, which drives retrograde enhancement of presynaptic function selectively at active presynaptic terminals.

Retrograde enhancement of presynaptic function requires new BDNF synthesis

Previous studies have demonstrated that rapid postsynaptic compensation at synapses induced by blocking miniature transmission is protein synthesis-dependent (Sutton et al., 2006, Aoto et al., 2008; see also, Ju et al., 2004), so we next examined whether the rapid presynaptic or postsynaptic changes associated with AMPAR blockade require new protein synthesis. As suggested by these earlier studies, we found that the rapid increase in surface GluA1 expression at synapses induced either by AMPAR blockade alone (3 hr CNQX), or AMPAR + AP blockade (CNQX + TTX), is prevented by the protein synthesis inhibitor anisomycin (40 μM, 30 min prior) (Figure 5A); a different translation inhibitor emetine (25 μM, 30 min prior) similarly blocked changes in sGluA1 induced by 3 hr CNQX treatment (data not shown). We also found (Figure 5B) that the state-dependent increase in syt-uptake induced by AMPAR blockade was prevented by pre-treatment (30 min prior to CNQX) with either anisomycin (40 uM) or emetine (25 uM). To verify that these changes in surface GluA1 expression and syt-lum uptake are indicative of changes in postsynaptic and presynaptic function, respectively, we examined the effects of anisomycin on mEPSCs (Figure 5C,D). In addition to preventing the enhancement of mEPSC amplitude, blocking protein synthesis prevented the state-dependent increase in mEPSC frequency induced by AMPAR blockade, suggesting that rapid homeostatic control of presynaptic function also requires new protein synthesis.

We next asked whether BDNF acts upstream or downstream of translation to persistently alter presynaptic function. BDNF has a well recognized role in enduring forms of synaptic plasticity via its ability to potently regulate protein synthesis in neurons (Kang and Schuman, 1996; Takei et al., 2001; Messaoudi et al., 2002; Tanaka et al., 2008), suggesting that BDNF release might engage the translation machinery to induce sustained changes in presynaptic function. If so, then like AMPAR blockade, the ability of BDNF to drive sustained presynaptic compensation should be prevented by protein synthesis inhibitors. Alternatively, BDNF itself could be a target of new protein synthesis, and could thus act as a translation effector induced by AMPAR blockade (e.g., Pang et al., 2004; Bekinschtein et al., 2007). If the role of BDNF is downstream of translation, it should recapitulate the enhancement of presynaptic function even in the presence of protein synthesis inhibitors. Indeed, we found that the time-course and magnitude of syt-lum uptake at excitatory synapses after BDNF treatment was virtually identical in the presence or absence of protein synthesis inhibitors (Figure 5E–F), despite the fact that these inhibitors completely prevent such increases induced by AMPAR blockade. These changes again were specific for the presynaptic compartment, since BDNF (250 ng/ml, 2 hrs) failed to alter postsynaptic surface GluA1 expression in the presence of anisomycin (data not shown). Moreover, the increase in mEPSC frequency induced by direct BDNF application was similarly unaffected by blocking protein synthesis with either anisomycin or emetine (Figure 5H–I). These results suggest that BDNF acts downstream of protein synthesis to drive state-dependent changes in presynaptic function.

Dendritic synthesis of BDNF accompanies AMPAR blockade

The results described above suggest that BDNF translation is a critical step in establishing state-dependent enhancement of presynaptic function during AMPAR blockade. To explore

this idea further, we examined whether AMPAR blockade alters BDNF expression. Western blotting of hippocampal neuron lysates after treatment with CNQX or APV demonstrated that AMPAR, but not NMDAR, blockade induces a time- dependent increase in BDNF expression (Figure 6A) that is blocked by anisomycin (Figure 6B), indicating that BDNF expression is up-regulated by AMPAR blockade in a protein synthesis-dependent manner. To examine whether BDNF expression after AMPAR blockade was differentially altered in specific sub-cellular compartments, we examined BDNF expression co-localized with specific pre- and postsynaptic markers by immunocytochemistry. We found that the increase in BDNF expression induced by AMPAR blockade was largely accounted for by regulation in dendrites, as MAP2-positive dendrites exhibited a significant increase in BDNF expression in neurons treated with CNQX (2 hrs), while somatic expression of BDNF from these same cells was unchanged (Figure 6C–G). Importantly, both dendritic and somatic MAP2 expression were similar between CNQX treated neurons and controls. These changes in dendritic BDNF expression were again specific to AMPAR blockade, since NMDAR blockade (APV, 2 hrs) failed to alter BDNF expression (Figure S8). In a parallel series of experiments, we found that AMPAR blockade failed to alter BDNF expression in neurofilament-positive axons or GFAP-positive astrocytes (Figure 6F and S8), indicating that AMPAR blockade induces an increase in neuronal BDNF expression that is specific to the dendritic compartment. Moreover, consistent with our biochemical data, the increase in dendritic BDNF expression induced by AMPAR blockade was due to *de novo* synthesis, since it was prevented by the translation inhibitors anisomycin and emetine (Figure 6F,G). Interestingly, blocking background spiking activity with TTX did not prevent the ability of AMPAR blockade to enhance dendritic BDNF expression in a protein synthesis-dependent manner (Figure 6H), suggesting that blockade of AP-independent miniature events are sufficient to drive changes in BDNF synthesis. Hence, while the downstream consequences of BDNF synthesis are gated by coincident activity in presynaptic terminals, the synthesis of BDNF appears more tightly linked with excitatory synaptic drive and the postsynaptic impact of miniature synaptic transmission.

Previous studies have documented the importance of local dendritic protein synthesis in forms of homeostatic plasticity induced, in whole or part, by targeting postsynaptic receptors with antagonists (Ju et al., 2005; Sutton et al., 2006; Aoto et al., 2008). Thus, the increase in dendritic BDNF expression could be due to localized dendritic synthesis or alternatively, due to somatic synthesis and subsequent transport into dendrites. It is well established that BDNF mRNA is localized to dendrites (Tongiorgi et al., 1997; An et al., 2008), and that miniature synaptic events regulate dendritic translation efficiency (Sutton et al., 2004), supporting the possibility that AMPAR blockade induces local BDNF synthesis in dendrites. To examine this possibility, we assessed the effects of locally blocking protein synthesis in dendrites using restricted microperfusion of emetine during global AMPAR blockade. When locally administered 15 min prior to and throughout bath CNQX treatment (40 μM; 60 min), emetine produced a selective decrease in dendritic BDNF expression in the presence of coincident bath CNQX application (Figure 7). Again, these local changes in BDNF expression were specific, as local administration of emetine had no effect on MAP2 expression in the same neurons, nor did local emetine have any effect on BDNF expression without coincident CNQX treatment (Figure 7D). These results thus indicate that the selective increase in dendritic BDNF expression induced by AMPAR blockade reflects localized dendritic BDNF synthesis. Taken together, our results suggest that AMPAR blockade induces local BDNF synthesis in dendrites which, in turn, selectively drives state-dependent compensatory increases in release probability from active presynaptic terminals.

DISCUSSION

We have shown that different facets of synaptic activity play unique roles in shaping the manner by which neurons homeostatically adjust pre- and postsynaptic function to compensate for acute loss of activity. In light of both the present findings and prior studies, we propose the following working mechanistic model (Figure 8) to explain the compensatory synaptic adaptations that accompany blockade of excitatory synaptic drive. AMPAR blockade induces two rapid and dissociable forms of synaptic compensation: 1) a postsynaptic increase in expression of GluA2-lacking AMPARs and a corresponding enhancement of mEPSC amplitude that is independent of background spiking activity, and 2) a retrograde enhancement of presynaptic function that is driven by the convergence of BDNF-TrkB signaling with AP-triggered Ca2+-influx through P/Q/N-type channels. Whereas the postsynaptic changes are sensitive to activity at either AMPARs or NMDARs, the enhancement in presynaptic function is unique to loss of AMPAR activity. Both pre- and postsynaptic changes require new protein synthesis, but appear to depend on distinct dendritically-synthesized protein products - GluA1 synthesis is likely critical for rapid postsynaptic compensation (Ju et al., 2004;Thiagarajan et al., 2005;Sutton et al., 2006;Aoto et al., 2008), while BDNF synthesis is critical for orchestrating retrograde compensatory changes in presynaptic function.

Retrograde Homeostatic Modulation of Presynaptic Function

Many studies have demonstrated postsynaptic forms of homeostatic compensation associated with enhanced expression of AMPARs at synapses (e.g., O'Brien et al., 1998; Wierenga et al., 2005; Sutton et al., 2006). However, clear evidence for homeostatic regulation of presynaptic neurotransmitter release has also been documented (e.g., Bacci et al., 2001; Murthy et al., 2001; Burrone et al., 2002; Thiagarajan et al., 2002; Wierenga et al., 2006; Branco et al., 2008). While methodological factors can contribute to this heterogeneity in expression (Wierenga et al., 2006), previous examples of retrograde effects of postsynaptic manipulations on presynaptic structure (e.g., Pratt et al., 2003) and function (e.g., Paradis et al., 2001; Burrone et al., 2003; Frank et al., 2006) suggest that intrinsic synaptic properties might also play a role. Indeed, we find that in addition to rapid postsynaptic effects, AMPAR blockade induces rapid (< 3 hr) functional compensation in the presynaptic compartment, an effect that is not observed with either acute (3 hr) or chronic (24 hr) AP blockade (see also, Bacci et al. 2001). Not only was AP blockade insufficient to produce changes in presynaptic function on its own, it also prevented AMPAR blockade from producing those changes. Hence, the compensatory increase in release probability induced by AMPAR blockade is state-dependent, requiring presynaptic spiking and P/Q/N-type Ca2+-channel function during the period of AMPAR blockade for its induction.

Our findings complement recent studies regarding retrograde homeostatic regulation of presynaptic neurotransmitter release. Frank and colleagues (2006) found that blocking spontaneous neurotransmission at the *Drosophila* NMJ induced rapid increases in presynaptic release probability; similar to our observations, they found that these changes were prevented by mutations in the presynaptic $Ca_V2.1$ channel encoded by the cacophony gene. The similar requirement for presynaptic voltage-gated Ca2+ channels in the two studies suggests that the state-dependent regulation of presynaptic function is evolutionarily conserved. Another recent study using hippocampal neurons (Branco et al., 2008) demonstrated that increases in local dendritic activity homeostatically decrease release probability from presynaptic terminals terminating on that dendrite. Our findings illustrate that the local homeostatic cross-talk between postsynaptic signaling and presynaptic release probability also operates in the opposite direction, where loss of postsynaptic activity selectively enhances release probability from active presynaptic terminals. Finally, whereas

our experiments focus on presynaptic changes induced by loss of synaptic input, data from Groth, Lindskog, Tsien and colleagues suggests that restoration of synaptic drive following activity blockade may also rapidly drive retrograde changes in release probability (Groth et al., 2009, Soc. Neurosci. Abs.). Hence, recent work from multiple groups establishes retrograde signaling as an important homeostatic mechanism in neural circuits.

BDNF as a state-dependent retrograde messenger

In our study, scavenging extracellular BDNF, blocking trkB activation, postsynaptic shRNA-mediated BDNF knockdown, and direct BDNF application all point to BDNF as a retrograde messenger linking postsynaptic consequences of AMPAR blockade with sustained enhancement of presynaptic neurotransmitter release. These results are consistent with previous studies showing that BDNF enhances presynaptic function (e.g., Lessman et al., 1994; Li et al., 1998; Schinder et al., 2000; Tyler and Pozzo-Miller, 2001) via a direct influence of BDNF signaling at the presynaptic terminal (Li et al., 1998; Pereira et al., 2006). In addition to BDNF, recent studies have demonstrated the importance of other releasable factors in homeostatic adjustment of synaptic strength. Stellwagen and Malenka (2006) demonstrated that glial-derived tumor-necrosis factor alpha (TNF-α) can drive postsynaptic compensation in neurons in response to chronic AP blockade. In our studies, glial cells do not seem to be the source of BDNF responsible for orchestrating presynaptic changes, since AMPAR blockade enhances BDNF synthesis in neuronal dendrites but does not influence BDNF expression in astrocytes. Interestingly, however, the role of TNF-α does seem to complement a more chronic role for BDNF in slow homeostatic adjustment of synaptic strength (Rutherford et al., 1998). In this study, co- treatment with BDNF prevented the gradual scaling of mEPSC amplitude induced by chronic TTX, whereas chronic treatment with a TrkB-IgG BDNF scavenger mimicked the slow scaling induced by TTX. Together with our results, these observations suggest that BDNF may have multiple time-dependent roles in homeostatic synaptic plasticity. Finally, a recent study (Aoto et al., 2008) has implicated the release of retinoic acid (RA) in orchestrating the synaptic incorporation of GluA2-lacking AMPARs to synapses induced by blocking miniature neurotransmission. Interestingly, while Aoto and colleagues (2008) demonstrate that RA mimics mini blockade in driving protein synthesis-dependent postsynaptic recruitment of GluA1 to synapses and enhancing mEPSC amplitude, it had no effect on mEPSC frequency suggesting a selective role in postsynaptic compensation. Together with our findings, these results suggest that distinct releasable factors may be engaged for homeostatic adjustment of pre- and postsynaptic function.

Multiple homeostatic modes control postsynaptic function

For homeostatic forms of plasticity induced by coincident blockade of APs and NMDARs, multiple studies have demonstrated enhanced synthesis of GluA1 in dendrites (Ju et al., 2004; Sutton et al., 2006) or synaptic fractions (Aoto et al., 2008), and the incorporation of GluA2-lacking receptors at synapses (Ju et al., 2004; Sutton et al., 2006; Aoto et al., 2008). By contrast, blockade of AP's alone induces a slower form of postsynaptic compensation characterized by enhanced expression of GluA2-containing AMPARs at synapses (Turrigiano et al., 1998; Wierenga et al., 2005; Sutton et al., 2006), possibly owing to a decrease in receptor removal and an accumulation of existing synaptic receptors (e.g., O'Brien et al., 1998; Ehlers, 2003; Ibata et al., 2008). These results support the notion that spontaneous and AP-mediated neurotransmission engage unique signaling pathways in neurons (Sutton et al., 2007; Atasoy et al., 2008) and that miniature synaptic events in these neurons play an important role in the acute homeostatic regulation of synaptic strength. Frank et al. (2006) identified a similar role for spontaneous neurotransmission in rapid homeostatic adjustment of synaptic function at the *Drosophila* neuromuscular junction, suggesting that this role for miniature events may be conserved across different synapse

classes and species. In a similar vein, Thiagarajan et al. (2005) demonstrated the synaptic recruitment of GluA2-lacking AMPARs in response to chronic (~24 hr) AMPAR blockade, suggesting that loss of AMPAR activity also engages mechanisms that recruit GluA2-lacking AMPARs to synapses. Our results extend these observations by demonstrating that AMPAR blockade induces rapid postsynaptic recruitment of GluA1 that is dependent on new protein synthesis. Moreover, we found that regardless of the presence or absence of background spiking, the increase in synaptic GluA1 and mEPSC amplitude induced by AMPAR blockade is indistinguishable. These results have two important implications. First, they demonstrate that while AP blockade reveals the functional impact of miniature neurotransmission (see also, Sutton et al., 2006), this role extends to conditions where background spiking is permissive. Second, they suggest that the rapid implementation of these postsynaptic changes is likely determined by changes in excitatory synaptic drive rather than postsynaptic firing rate, since AP blockade alone induces a distinct set of postsynaptic changes (i.e., enhanced expression of GluA2-containing AMPARs) with far slower kinetics (> 12 hr; Turrigiano et al., 1998; Wierenga et al., 2005; Sutton et al., 2006). This notion is further supported by the observation that spatially-restricted blockade of NMDAR miniature events enhances surface GluA1 expression locally (Sutton et al., 2006). While these observations and some theoretical considerations (Rabinowitch and Segev, 2008) argue for a local homeostatic mechanism, there is also strong evidence for more global homeostatic control mechanisms in neurons that may be tuned to firing rate (Turrigiano et al., 1998). There are unique theoretical advantages of global homeostatic mechanisms as well, particularly with regard to preserving information coding capabilities of neurons (Turrigiano, 2008). A recent study directly assessed the impact of blocking postsynaptic firing by confining TTX treatment to the postsynaptic cell body. Ibata et al. (2008) found such somatic AP blockade induced a transcription-dependent accumulation of GFP-tagged GluA2 at multiple sites throughout the dendritic arbor remote from the perfusion site, indicative of a cell-wide homeostatic mechanism. This transcription-dependent connection adds an interesting parallel with other evidence implicating the immediate early gene Arc in global homeostatic control (Shepherd et al., 2006), and also distinguishes this global mechanism with transcription-independent synaptic insertion of GluA2-lacking receptors that accompanies mini blockade (Aoto et al., 2008). Taken together, these observations support the existence of multiple modes of homeostatic control in neurons that are mediated by separate molecular pathways and implemented over distinct spatial scales.

Dendritic BDNF synthesis drives local changes in presynaptic function

Since the discovery of polyribosomes beneath synaptic sites on dendrites, the hypothesis that dendritic protein synthesis can be engaged to adjust synaptic composition on a local level has received considerable attention. Our results indicate that in addition to allowing for fine spatial control over the postsynaptic element, local dendritic synthesis may also actively participate in controlling the function of apposed presynaptic terminals, through local synthesis of BDNF and perhaps other retrograde messengers. Thus, BDNF is both necessary and sufficient for the state-dependent presynaptic changes induced by AMPAR blockade, but acts downstream of protein synthesis. Furthermore, AMPAR blockade enhances dendritic BDNF expression in a translation-dependent manner, and a local decrease in dendritic BDNF expression accompanies spatially-restricted inhibition of dendritic protein synthesis when performed coincident with AMPAR blockade. This latter result suggests that the mobility of the BDNF pool synthesized in response to AMPAR blockade is restricted, although it is not presently clear what mechanisms are responsible. Future studies examining dynamic BDNF synthesis and trafficking in dendrties will be useful in elucidating mechanisms that are responsible for this restricted mobility. Importantly, preventing spiking in synaptic terminals or the $Ca2^{+}$ influx triggered by spiking completely prevents the

sustained presynaptic changes induced by BDNF, but does not appear to affect the synthesis of BDNF directly. Hence, we conclude that a dendritic source of BDNF participates in enhancing release probability at apposed presynaptic sites, but only at active terminals. It is now of interest to determine how BDNF-driven signaling interacts with signaling driven by AP-triggered $Ca2^{+}$ influx in presynaptic terminals to mediate this state-dependent enhancement of presynaptic function.

BDNF has received considerable attention for its role in long-lasting synaptic plasticity and memory. Much of this interest is driven by the fact that BDNF is known to potently regulate neuronal translation generally (e.g., Takei et al., 2001), and local translation in dendrites in particular (e.g., Aakalu et al., 2001; Yin et al., 2002). Furthermore, there is substantial evidence that one critical role of BDNF in long-term plasticity is for inducing translation, i.e., BDNF acts upstream of protein synthesis for certain forms of LTP (e.g., Kang and Schuman, 1996; Messaoudi et al., 2002; Tanaka et al., 2008). However, evidence has been emerging that BDNF may play distinct roles downstream of protein synthesis, presumably via its own translation (Pang et al., 2004; Bekinschtein et al., 2007). Given that BDNF can act both upstream and downstream of protein synthesis, a critical issue is what unique functional contributions BDNF might make in these different roles. Collectively, our results suggest one important aspect of BDNF's role as a translation effector is to orchestrate presynaptic changes in a state-dependent manner. For homeostatic plasticity, this role of BDNF has the important consequence of coordinating compensatory changes at postsynaptic sites with corresponding increases in presynaptic function. This specific role may well extend beyond homeostatic compensation, and the importance of BDNF as a translation effector in long-term potentiation (Pang et al., 2004) and memory (Bekinschtein et al., 2007) could relate to its ability to enhance presynaptic function in a state-dependent manner. Although this notion remains speculative, the fact that active presynaptic terminals are uniquely sensitive to BDNF's effects suggests that in other contexts, BDNF could provide feedback to presynaptic terminals in a Hebbian fashion. In other words, our results predict that inputs that are activated in an experience-dependent fashion, as might occur during repetitive training trials, will be selectively strengthened via the state-dependent enhancement of presynaptic function conferred by BDNF. This type of mechanism could, in principle, allow for plasticity mechanisms that are initially confined to the postsynaptic compartment to engage appropriate synaptic contacts and drive coordinate changes in their function so as to effectively match efficacy on both sides of the synapse.

EXPERIMENTAL PROCEDURES

Cell Culture and Electrophysiology

Dissociated postnatal (P0–2) rat hippocampal neuron cultures were prepared as previously described (Sutton et al., 2006). mEPSCs were recorded from a holding potential of − 70 mV with an Axopatch 200B amplifier from neurons bathed in HEPES-buffered saline (HBS; containing, in mM: 119 NaCl, 5 KCl, 2 $CaCl_2$, 2 $MgCl_2$, 30 Glucose, 10 HEPES, pH 7.4 plus 1 μM TTX and 10 μM bicuculine; mEPSCs were analyzed with Synaptosoft minianalysis software. For paired-pulse facilitation experiments, evoked EPSCs were elicited with 0.3 ms pulses delivered by an extracellular bipolar stimulating electrode positioned near the recorded neuron. All PPF experiments were conducted in HBS with 0.5 $CaCl_2$ and 3.5 $MgCl_2$ within 15 min of CNQX or CNQX/TTX washout. Whole-cell pipette internal solutions contained, in mM: 100 cesium gluconate, 0.2 EGTA, 5 $MgCl_2$, 2 ATP, 0.3 GTP, 40 HEPES, pH 7.2. Statistical differences between experimental conditions were determined by ANOVA and post-hoc Fisher's LSD test.

BDNF shRNA Transfection

U6 promotor-driven scrambled and BDNF shRNA-expressing plasmids were obtained from OriGene Technologies (Rockville, MD); BDNF shRNA 1: 5′-TGTTCCACCAGGTGAGAAGAGTGATGACC-3, BDNF shRNA 2: 5′-GTGATGCTCAGCAGTCAAGTGCCTTTGGA-3′, scrambled: 5′-GCACTACCAGAGCTAACTCAGATAGTACT-3′. Each plasmid additionally contains a tRFP expression cassette driven by a distinct (pCMV) promoter. Neurons were transfected with 0.5 μg of total DNA using the CalPhos Transfection kit (ClonTech; Mountain View, CA) according to the manufacturer's protocol. All experiments were performed 24 hr post transfection.

Western Blotting

Samples were collected in lysis buffer containing, in mM: 100 NaCl, 10 $NaPO_4$, 10 $Na_4P_2O_7$, 10 lysine, 5 EDTA, 5 EGTA, 50 NaF, 1 $NaVO_3$, 1% Triton-X, 0.1% SDS, 1 tablet Complete Mini protease inhibitor cocktail (Roche)/7 ml, pH 7.4. Equal amounts of protein for each sample were loaded and separated on 12% polyacrylamide gels, then transferred to PVDF membranes. Blots were blocked with Tris-buffered saline containing 0.1 % Triton-X (TBST) and 5% non-fat milk for 60 min at RT, and incubated with a rabbit polyclonal primary antibody against BDNF (Santa Cruz, 1: 200) for either 60 min at RT or overnight at 4°C. After washing with TBST, blots were incubated with HRP-conjugated anti-rabbit secondary antibody (1:5000; Jackson Immunoresearch) followed by chemiluminescent detection (ECL, Amersham Biosciences). The same blots were re-probed with a mouse monoclonal antibody against α-tubulin (1:5000, Sigma) to confirm equal loading. Band intensity was quantified with densitometry using NIH image J, and expressed relative to the matched control sample. Statistical differences between treatment conditions and control were assessed by Chi square, whereas comparisons between CNQX and CNQX + anisomycin were assessed with an unpaired t-test (two-tailed).

Immunocytochemisty and Microscopy

Surface GluA1 (sGluA1) was labeled and imaged as described previously (Sutton et al., 2006). Live-labeling (5 min) with an Oyster 550-conjugated rabbit polyclonal antibody against the lumenal domain of synaptotagmin 1 (syt-lum; 1:100, Synaptic Systems) was used to assess presynaptic function. Prior to labeling, neurons were treated with 2 μM TTX for 15 min to isolate spontaneous neurotransmitter release. Synaptic terminals were identified in the same samples using either a mouse monoclonal antibody against bassoon (1:1000, Stressgen) or a guinea pig polyclonal anti-vglut1 antibody (1: 2500, Chemicon). For BDNF staining, cells were fixed on ice for 30 min with 4% paraformaldehyde (PFA)/4% sucrose in phosphate buffered saline with 1 mM $MgCl_2$ and 0.1 mM $CaCl_2$ (PBS-MC), permeabilized (0.1 % Triton X in PBS-MC, 5 min), blocked with 2% bovine serum albumin (BSA) in PBS-MC for 30 min, and labeled with a rabbit polyclonal antibody against BDNF (Santa Cruz, 1:100). For co-labeling of dendrites, axons, and astrocytes, respectively, we used the following: a mouse monoclonal antibody against MAP2 (Sigma, 1:5000), a pan-axonal neurofilament mouse monoclonal antibody cocktail (1:8000, clone SMI-312, Covance), and a mouse monoclonal antibody against GFAP (Sigma, 1:1000). Secondary detection was achieved with Alexa 488-, 555-, or 635-conjugated goat anti-rabbit or goat anti-mouse antibodies for 60 min at RT

All imaging was performed on an inverted Olympus FV1000 laser scanning confocal microscope using identical acquisition parameters for each treatment condition. Image analysis was performed on maximal intensity z-projected images. For analysis of sGluA1 or syt-lum staining, a "synaptic" particle was defined as occupying greater than 10% of the area defined by a PSD95 or vglut1/bassoon particle. Analysis was performed using custom

written analysis routines for Image J. Statistical differences were assessed by ANOVA, followed by Fisher's LSD post-hoc tests.

Local Perfusion

Stable microperfusion was achieved by use of a dual micropipette delivery system, as described (Sutton et al., 2006). A cell-impermeant fluorescent dye (either Alexa 488 or Alexa 555 hydrazide, 1 μg/ml) was included in the local perfusate to visualize the affected area. In all local perfusion experiments, the bath was maintained at 37°C and continuously perfused at 1.5 ml/min with HBS. For analysis, the size of the treated area was determined in each linearized dendrite based on Alexa 488/555 fluorescence integrated across all images taken during local perfusion. Adjacent non-overlapping dendritic segments, 25 μm in length, proximal and distal to the treated area were assigned negative and positive values, respectively. For experiments examining local regulation of BDNF expression, the average non-zero pixel intensity for the entire length of dendrite, excluding the treated area, was used to normalize BDNF intensity. For experiments examining syt-lum uptake, immediately following local perfusion, 2 μM TTX was bath applied for 10 min to isolate spontaneous neurotransmitter release. Neurons were then live labeled with anti-syt-lum for 5 min at RT, and processed for immunocytochemistry as described above. The density and intensity of vglut particles were calculated for each dendritic segment, and the average value was then used to normalize vlgut density and intensity in all segments (including the treated area). The proportion of vglut particles with syt-lum particles was also determined in each segment. Statistical differences were assessed by ANOVA and Fisher's LSD post-hoc tests.

Supplementary Material

Refer to Web version on PubMed Central for supplementary material.

Acknowledgments

We thank Richard Tsien, Mia Lindskog, and Rachel Groth for their helpful comments on the manuscript, as well as Hisashi Umemori and members of the Sutton lab for useful discussions. This work was supported by RO1MH085798 from The National Institute of Mental Health (M.A.S.) and a grant from the Pew Biomedical Scholars Program (M.A.S.).

References

Aakalu G, Smith WB, Jiang C, Nguyen N, Schuman EM. Dynamic visualization of dendritic protein synthesis in hippocampal neurons. Neuron 2001;30:489–502. [PubMed: 11395009]

Alder J, Thakker-Varia S, Crozier RA, Shaheen A, Plummer MR, Black IB. Early presynaptic and late postsynaptic components contribute independently to brain-derived neurotrophic factor-induced synaptic plasticity. J Neurosci 2005;25:3080–3085. [PubMed: 15788764]

An JJ, Gharami K, Liao GY, Woo NH, Lau AG, Vanevski F, Torre ER, Jones KR, Feng Y, Lu B, Xu B. Distinct role of long 3′ UTR BDNF mRNA in spine morphology and synaptic plasticity in hippocampal neurons. Cell 2008;134:175–187. [PubMed: 18614020]

Aoto J, Nam CI, Poon MM, Ting P, Chen L. Synaptic signaling by all-trans retinoic acid in homeostatic synaptic plasticity. Neuron 2008;60:308–320. [PubMed: 18957222]

Atasoy D, Ertunc M, Moulder KL, Blackwell J, Chung C, Su J, Kavalili E. Spontaneous and evoked glutamate release activates two populations of NMDA receptors with limited overlap. J Neurosci 2008;28:10151–10166. [PubMed: 18829973]

Bacci A, Coco S, Pravettoni E, Schenk U, Armano S, Frassoni C, Verderio C, De Camilli P, Matteoli M. Chronic blockade of glutamate receptors enhances presynaptic release and downregulates the interaction between synaptophysin-synaptobrevin-vesicle-associated membrane protein 2. J Neurosci 2001;21:6588–6596. [PubMed: 11517248]

Bekinschtein P, Cammarota M, Igaz LM, Bevilaqua LR, Izquierdo I, Medina JH. Persistence of long-term memory storage requires a late protein synthesis- and BDNF-dependent phase in the hippocampus. Neuron 2007;53:261–277. [PubMed: 17224407]

Branco T, Staras K, Darcy KJ, Goda Y. Local dendritic activity sets release probability at hippocampal synapses. Neuron 2008;59:475–485. [PubMed: 18701072]

Burrone J, O'Byrne M, Murthy VN. Multiple forms of synaptic plasticity triggered by selective suppression of activity in individual neurons. Nature 2002;420:414–418. [PubMed: 12459783]

Davis GW. Homeostatic control of neural activity: from phenomenology to molecular design. Ann Rev Neurosci 2006;29:307–323. [PubMed: 16776588]

Echegoyen J, Neu A, Graber KD, Soltesz I. Homeostatic plasticity studied using in vivo hippocampal activity-blockade: synaptic scaling, intrinsic plasticity, and age-dependence. PLoS ONE 2007;2:e700. [PubMed: 17684547]

Ehlers MD. Activity level controls postsynaptic composition and signaling via the ubiquitin-proteasome system. Nat Neurosci 2003;6:231–242. [PubMed: 12577062]

Frank CA, Kennedy MJ, Goold CP, Marek KW, Davis GW. Mechanisms underlying the rapid induction and sustained expression of synaptic homeostasis. Neuron 2006;52:663–677. [PubMed: 17114050]

Gong B, Wang H, Gu S, Heximer SP, Zhuo M. Genetic evidence for the requirement of adenylyl cyclase 1 in synaptic scaling of forebrain cortical neurons. Eur J Neurosci 2007;26:275–288. [PubMed: 17650106]

Ibata K, Sun Q, Turrigiano GG. Rapid synaptic scaling induced by changes in postsynaptic firing. Neuron 2008;57:819–826. [PubMed: 18367083]

Ju W, Morishita W, Tsui J, Gaietta G, Deerink TJ, Adams SR, Garner CC, Tsien RY, Ellisman MH, Malenka RC. Activity-dependent regulation of dendritic synthesis and trafficking of AMPA receptors. Nat Neurosci 2004;7:244–253. [PubMed: 14770185]

Kang H, Schuman EM. A requirement for local protein synthesis in neurotrophin-induced synaptic plasticity. Science 1996;273:1402–1406. [PubMed: 8703078]

Lessman V, Gottman K, Heumann R. BDNF and NT-4/5 enhance glutamatergic synaptic transmission in cultured hippocampal neurons. Neuroreport 1994;6:21–25. [PubMed: 7703418]

Li YX, Xu Y, Ju D, Lester HA, Davidson N, Schuman EM. Expression of a dominant negative TrkB receptor, T1, reveals a requirement for presynaptic signaling in BDNF-induced synaptic potentiation in cultured hippocampal neurons. Proc Natl Acad Sci USA 1998;95:10884–10889. [PubMed: 9724799]

Messaoudi E, Ying SW, Kanhema T, Croll SD, Bramham CR. Brain-derived neurotrophic factor triggers transcription-dependent, late phase long-term potentiation in vivo. J Neurosci 2002;22:7453–7461. [PubMed: 12196567]

Murthy VN, Schikorski T, Stevens CF, Zhu Y. Inactivity produces increases in neurotransmitter release and synapse size. Neuron 2001;32:673–682. [PubMed: 11719207]

O'Brien RJ, Kamboj S, Ehlers MD, Rosen KR, Fischbach GD, Huganir RL. Activity-dependent modulation of synaptic AMPA receptor accumulation. Neuron 1998;21:1067–1078. [PubMed: 9856462]

Pang P, Teng HK, Zaitsev E, Woo NT, Sakata K, Zhen S, Teng KK, Yung W, Hempstead BL, Lu B. Cleavage of proBDNF by tPA/Plasmin is essential for long-term hippocampal plasticity. Science 2004;306:487–491. [PubMed: 15486301]

Paradis S, Sweeney ST, Davis GW. Homeostatic control of presynaptic release is triggered by postsynaptic membrane deplolarization. Neuron 2001;30:737–749. [PubMed: 11430807]

Pereira DB, Rebola N, Rodrigues RJ, Cunha RA, Carvalho AP, Duarte CB. TrkB receptor modulation of glutamate release is limited to a subset of nerve terminals in the adult rat hippocampus. J Neurosci Res 2006;83:832–844. [PubMed: 16477614]

Pozo K, Goda Y. Unraveling mechanisms of homeostatic synaptic plasticity. Neuron 2010;66:337–351. [PubMed: 20471348]

Pratt KG, Watt AJ, Griffith LC, Nelson SB, Turrigiano GG. Activity-dependent remodeling of presynaptic inputs by postsynaptic expressionof activated CaMKII. Neuron 2003:269–281. [PubMed: 12873384]

Rabinowitch I, Segev I. Two opposing plasticity mechanisms pulling a single synapse. Trends Neurosci 2008;31:377–383. [PubMed: 18602704]

Rutherford LC, Nelson SB, Turrigiano GG. BDNF has opposite effects on the quantal amplitude of pyramidal neuron and interneuron excitatory synapses. Neuron 1998;21:521–530. [PubMed: 9768839]

Schinder AF, Berninger B, Poo M. Postsynaptic target specificity of neurotophin-induced presynaptic potentiation. Neuron 2000;25:151–163. [PubMed: 10707980]

Shepherd JD, Rumbaugh G, Wu J, Chowdhury S, Plath N, Kuhl D, Huganir RL, Worley PF. Arc/Arg3.1 mediates homeostatic synaptic scaling of AMPA receptors. Neuron 2006;52:475–484. [PubMed: 17088213]

Stellwagen D, Malenka R. Synaptic scaling mediated by glial TNF-alpha. Nature 2006;440:1054–1059. [PubMed: 16547515]

Sutton MA, Wall NR, Aakalu GN, Schuman EM. Regulation of dendritic protein synthesis by miniature synaptic events. Science 2004;304:1979–1983. [PubMed: 15218151]

Sutton MA, Ito HT, Cressy P, Kempf C, Woo JC, Schuman EM. Miniature neurotransmission stabilizes synaptic function via tonic suppression of local dendritic protein synthesis. Cell 2006;125:785–799. [PubMed: 16713568]

Sutton MA, Taylor AM, Ito HT, Pham A, Schuman EM. Postsynaptic decoding of neural activity: eEF2 as a biochemical sensor coupling miniature synaptic transmission to local protein synthesis. Neuron 2007;55:648–661. [PubMed: 17698016]

Takei N, Kawamura M, Hara K, Yonezawa K, Nawa H. Brain-derived neurotrophic factor enhances neuronal translation by activating multiple initiation processes: comparison with the effects of insulin. J Biol Chem 2001;276:42818–42825. [PubMed: 11551908]

Tanaka J, Horiike Y, Masuzaki M, Miyazaki T, Ellis-Davies GC, Kasai H. Protein synthesis and neurotophin-dependent structural plasticity at single dendritic spines. Science 2008;319:1683–1687. [PubMed: 18309046]

Thiagarajan TC, Lindskog M, Tsien RW. Adaptation to synaptic inactivity in hippocampal neurons. Neuron 2005;47:725–737. [PubMed: 16129401]

Tongiorgi E, Righi M, Cattaneo A. Activity-dependent dendritic targeting of BDNF and TrkB mRNAs in hippocampal neurons. J Neurosci 1997;17:9492–9505. [PubMed: 9391005]

Turrigiano GG. The self-tuning neuron: synaptic scaling of excitatory synapses. Cell 2008;135:422–435. [PubMed: 18984155]

Turrigiano GG, Leslie KR, Desai NS, Rutherford LC, Nelson SB. Activity-dependent scaling of quantal amplitude in neocortical neurons. Nature 1998;391:892–896. [PubMed: 9495341]

Tyler WJ, Pozzo-Miller LD. BDNF enhances quantal neurotransmitter release and increases the number of docked vesicles at the active zones of hippocampal excitatory synapses. J Neurosci 2001;21:4249–4258. [PubMed: 11404410]

Wheeler DB, Randall A, Tsien RW. Roles of N-type and Q-type Ca2+ channels in supporting hippocampal synaptic transmission. Science 1994;264:107–111. [PubMed: 7832825]

Wierenga CJ, Ibata K, Turrigiano GG. Postsynaptic expression of homeostatic plasticity at neocortical synapses. J Neurosci 2005;25:2895–2905. [PubMed: 15772349]

Wierenga CJ, Walsh MF, Turrigiano GG. Temporal regulation of the expression locus of homeostatic plasticity. J Neurophysiol 2006;96:2127–2133. [PubMed: 16760351]

Yin Y, Edelman GM, Vanderklish PW. The brain-derived neurotrophic factor enhances synthesis of Arc in synaptoneurosomes. Proc Natl Acad Sci USA. 2002

Zhang XH, Poo MM. Localized synaptic potentiation by BDNF requires local protein synthesis in the developing axon. Neuron 2002;36:675–688. [PubMed: 12441056]

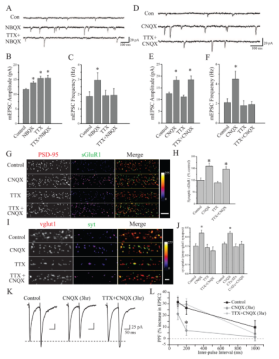

Figure 1. AMPAR blockade induces a state-dependent enhancement of presynaptic function

(A–C) Representative recordings (A) and mean (+ SEM) mEPSC amplitude (B) and frequency (C) of experiments (27–40 DIV) from the following conditions (24 hr): Control (n = 13), 10 μM NBQX (n = 9), 2 μM TTX (n = 10), TTX+NBQX (n = 8). 24 hr NBQX increases both mEPSC amplitude and frequency (*p < 0.05, relative to control); AP blockade prevents the increase in mEPSC frequency induced by AMPAR blockade, but not changes in mEPSC amplitude. (D–F) Representative recordings (D) and mean (+ SEM) mEPSC amplitude (E) and frequency (F) of experiments (21–38 DIV) from the following conditions (3 hr): Control (n = 10), 40 μM CNQX (n = 12), 2 μM TTX (n = 10), and TTX +CNQX (n = 11). Brief AMPAR blockade induces a significant (*p < 0.05, relative to control) increase in both mEPSC amplitude and frequency; AP blockade prevents the increase in mEPSC frequency induced by AMPAR blockade, but not changes in mEPSC amplitude. (G) Representative examples and (H) mean (+SEM) normalized surface GluA1 expression at excitatory synapses (21–40 DIV) from the following conditions (3 hr): Controls (n = 46), CNQX (n = 44), TTX (n = 48), or CNQX+TTX (n = 46). Brief AMPAR blockade significantly (*p < 0.05, relative to control) enhances postsynaptic surface GluA1 expression in the presence or absence of background spiking. (I–J) Representative examples and mean (+SEM) proportion of vglut1-positive excitatory presynaptic terminals with corresponding syt-lum signal from the indicated treatment groups (DIV 37–40). Left to right n = 54, 49, 52, 50, 64, 68, 64, 67 images. Brief AMPAR blockade significantly (*p < 0.05, relative to control) enhances synaptic syt-lum uptake which is prevented by coincident AP (+TTX) or P/Q/N-Ca2+ channel (+CTx/ATx) blockade. (K) Example traces and (L) mean (± SEM) paired-pulse facilitation (PPF), defined as the percent increase in peak amplitude of EPSC2 relative to EPSC1 at different inter-pulse intervals. AMPAR blockade (CNQX alone; n = 29 neurons) produced a significant (*p < 0.05, relative to control; n = 29 neurons) decrease in PPF; co-application of TTX during AMPAR blockade (n = 29 neurons) restored PPF to control levels. The dashed line represents peak amplitude of EPSC1. Scale bars = 25 pA, 50 ms.

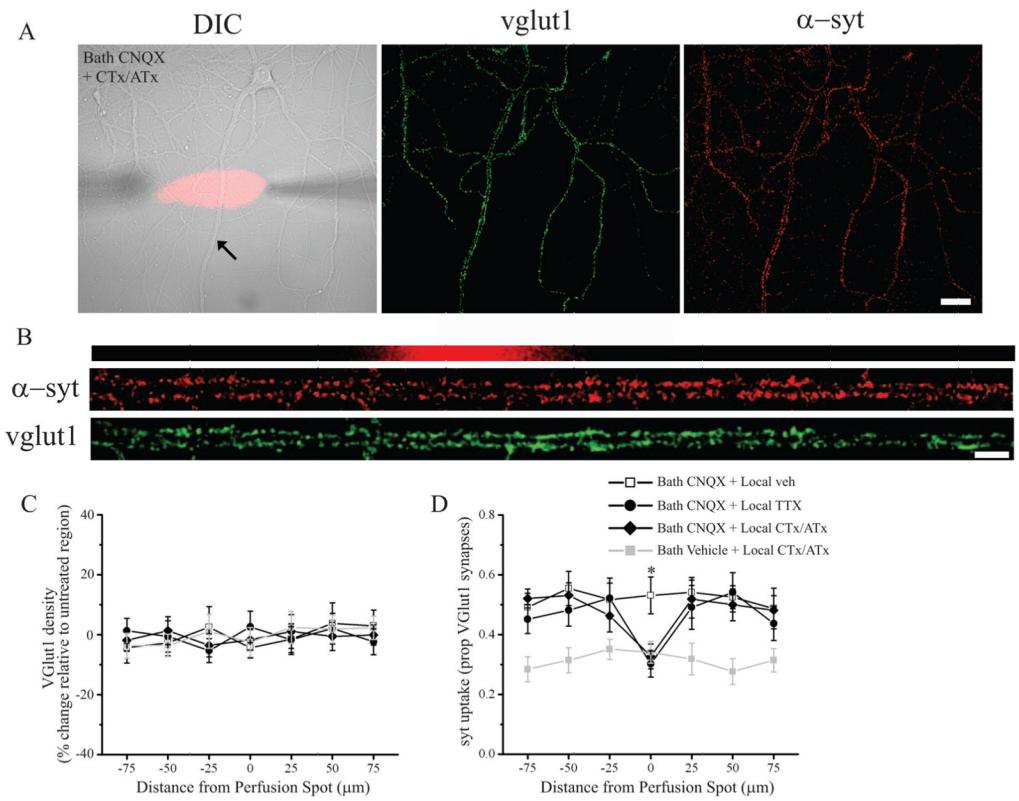

Figure 2. Local presynaptic activity gates retrograde enhancement of presynaptic function induced by AMPAR blockade

(A) Representative DIC image (24 DIV) with superimposed CTx/ATx perfusion spot (red) and syt-lum and vglut1 staining from the same neuron. (B) Linearized dendrite indicated by the arrow shown in (A) with corresponding syt-lum and vglut1 staining registered to the perfusion area (red). Scale bar = 30 μm and 10 μm in (A) and (B), respectively. (C–D) Analysis of group data. On the abscissa, positive and negative values indicate, respectively, segments distal and proximal from the treated area. (C) Mean (± SEM) normalized vglut1 density in treated and untreated dendritic segments; local perfusion did not affect synaptic density. (D) Mean (± SEM) proportion of vglut1-positive synapses with corresponding syt-lum signal in treated and untreated dendritic segments. Coincident AMPAR blockade (20 μM CNQX, 2 hrs) significantly (* $p < 0.05$) increased syt uptake in the treated area in neurons locally treated with vehicle relative to those locally treated with TTX or CTx/ATx. For the groups indicated from top to bottom in (D), n = 10 dendrites from 7 cells; 12 dendrites from 8 cells; 14 dendrites from 10 cells; 11 dendrites from 7 cells (21–35 DIV).

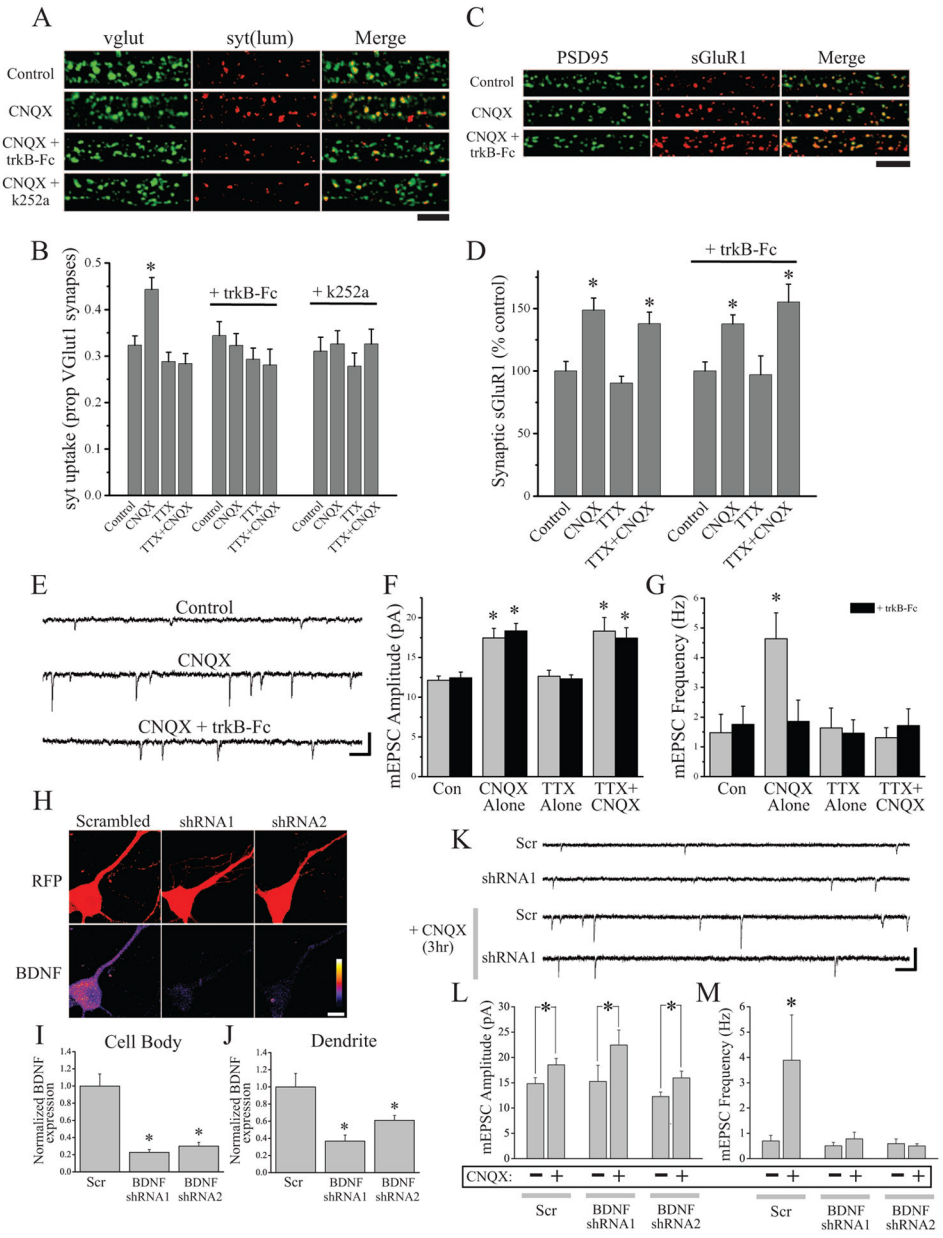

Figure 3. BDNF release and signaling are required for presynaptic, but not postsynaptic, compensation induced by AMPAR blockade

(A) Representative examples and (B) mean (+ SEM) syt-lum uptake from experiments (25 DIV) where the indicated treatment groups were examined either alone (n = 34 images/group) or co-treated (30 min prior) with trkB-Fc (1 μg/ml; n = 38 images/group) or k252a (100 nM; n = 24 images/group). Scavenging extracellular BDNF (trkB-Fc) or blocking BDNF-induced signaling (k252a) each blocked enhanced syt-lum uptake induced by AMPAR blockade (*$p < 0.05$, relative to control). (C) Representative examples and (D) mean (+ SEM) normalized synaptic sGluA1 expression in the indicated groups (25 DIV). For the groups indicated from left to right, n = 32, 30, 32, 31, 31, 32, 32, 32 images. BDNF is not required for enhanced synaptic GluA1 expression following AMPAR blockade. Scale bars = 5 μm and 10 μm in (A) and (C), respectively. (E) Representative recordings (scale bar = 20 pA, 200 ms) and mean (+ SEM) mEPSC amplitude (F) and frequency (G) in neurons

(21–42 DIV) after the indicated treatments either with or without 30 min pre-incubation with 1 μg/ml trkB-Fc. For the indicated groups: control (n = 8, 10), CNQX (n = 11, 12), TTX (n = 8, 8), TTX+CNQX (n = 10, 9). Treatment with trkB-Fc blocked the increase in mEPSC frequency but not the increase in mEPSC amplitude induced by AMPAR blockade. (H–J) Example images (H) and mean (+ SEM) normalized BDNF expression in cell bodies (I) and dendrites (J) of transfected neurons. Scale bar = 10 μm; *$p < 0.05$ vs. scrambled control. (K–M) Representative recordings (K) and mean (+ SEM) mEPSC amplitude (L) and frequency (M) in neurons (21–42 DIV) transfected with either a scrambled control shRNA (Scr) or shRNAs against BDNF. Scale bar = 15 pA, 400 ms. Mean (+ SEM) mEPSC amplitude (L) and frequency (M) in neurons (21–42 DIV) transfected with scrambled shRNA or shRNAs against BDNF. Postsynaptic BDNF knockdown prevents the increase in mEPSC frequency (but not amplitude) following AMPAR blockade (CNQX, 3 hrs).

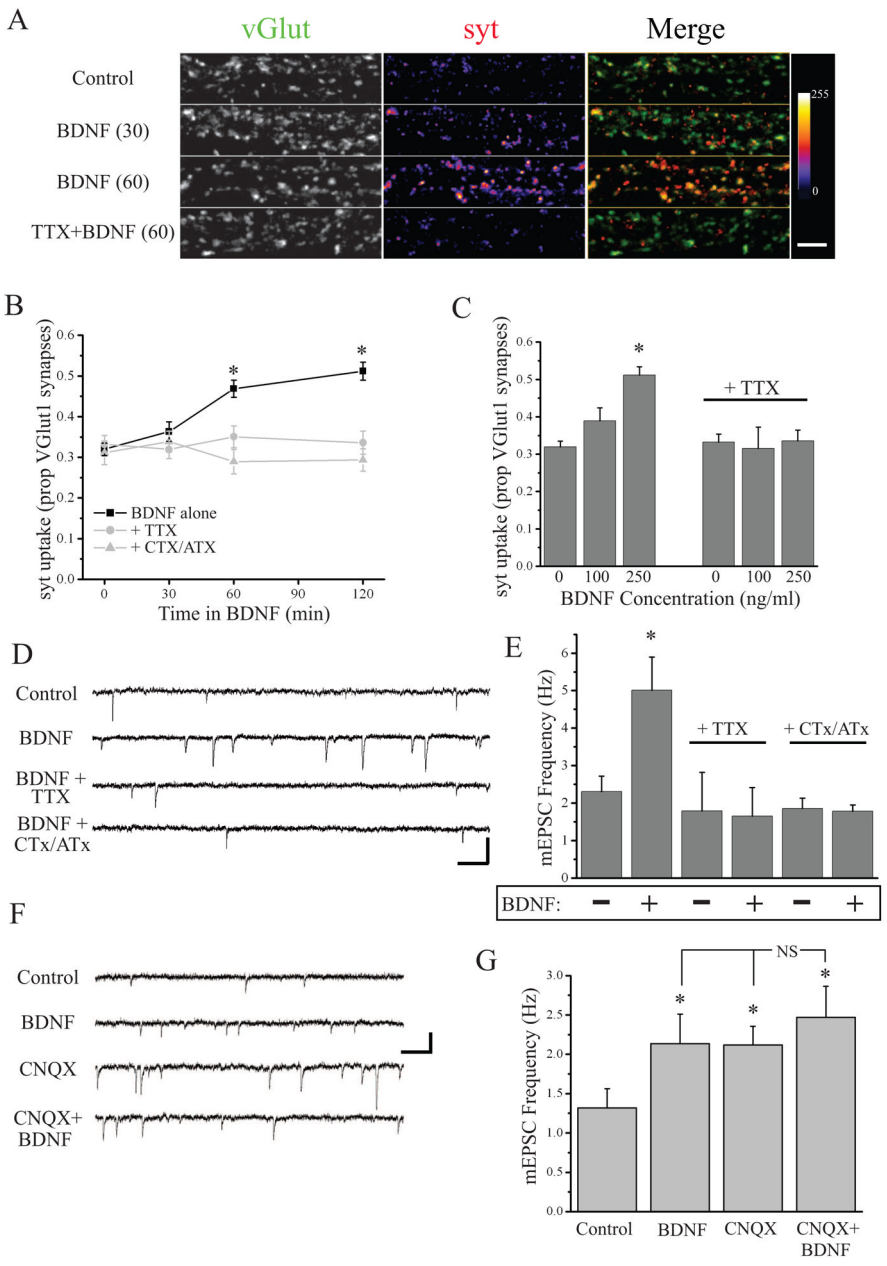

Figure 4. BDNF enhances presynaptic function in a state-dependent manner

(A) Representative examples and (B) mean (± SEM) spontaneous syt-lum uptake from neurons (25–43 DIV) following incubation with BDNF (250 ng/ml) for the indicated times. Color-look up table indicates syt fluorescence intensity; scale bar = 10 μm. BDNF increased spontaneous syt-lum uptake at synapses (*$p < 0.05$, relative to 0 min); coincident treatment with TTX or CTx/ATx completely prevents this effect. (C) Mean (+ SEM) state-depdendent syt-lum uptake as a function of BDNF (2 hr) concentration (* $p < 0.05$ relative control). (D) Representative recordings (scale bar = 20 pA, 200 ms) and (E) mean (+ SEM) mEPSC frequency in neurons (21–51 DIV) treated with BDNF (250 ng/ml, 2 hrs) either alone or coincident with TTX or CTx/ATx. BDNF significantly (* $p < 0.05$ relative control) increases mEPSC frequency which is prevented by AP or P/Q/N-Ca2+ channel blockade. (F) Representative recordings (scale bar = 15 pA, 200 ms) and (G) mean (+ SEM) mEPSC

frequency in neurons (21–42 DIV) treated as follows: control (n = 12), BDNF (250 ng/ml, 2 hrs; n = 12), CNQX (40 μM, 3 hrs; n = 12), BDNF+CNQX (n = 8) prior to TTX application and mEPSC recording. Both BDNF and CNQX produce a significant (* $p < 0.05$ relative control) increase in mEPSC frequency, but the combination of the two does not produce a significant additive effect.

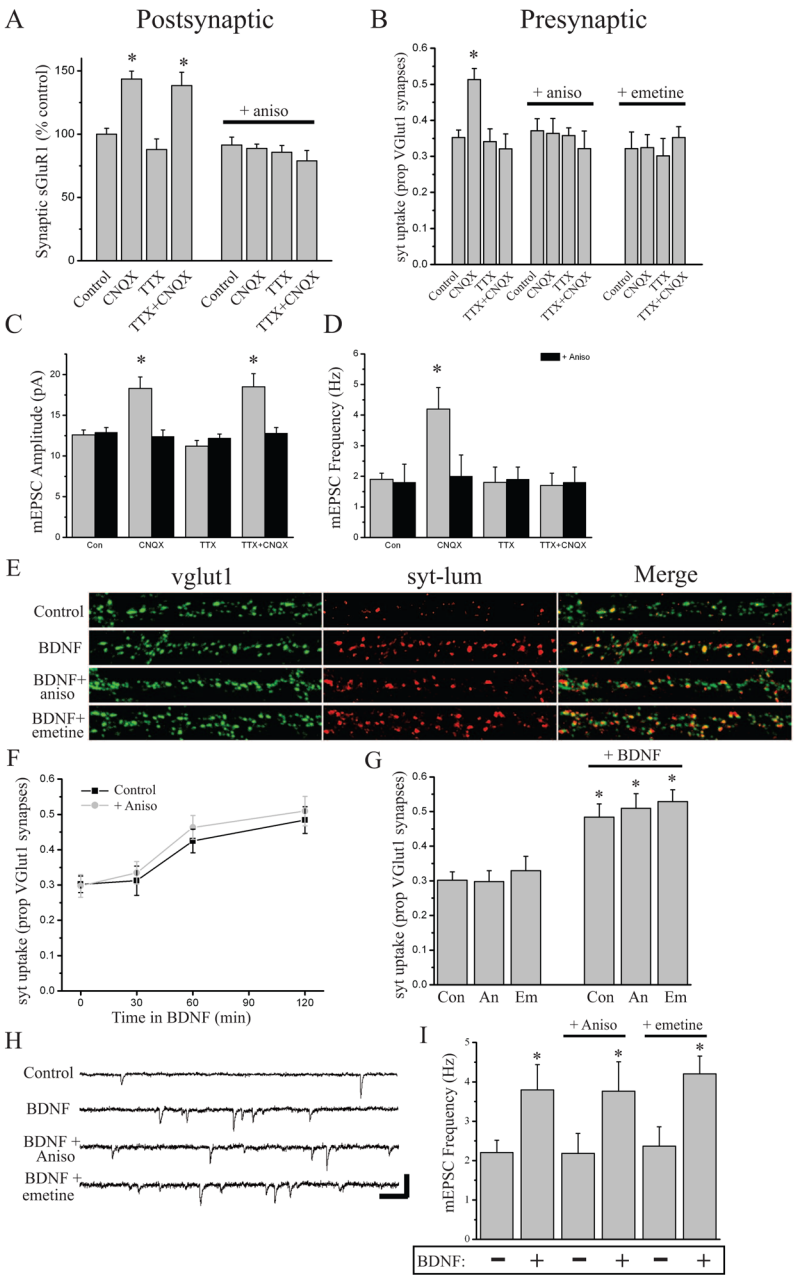

Figure 5. BDNF acts downstream of protein synthesis to enhance presynaptic function induced by AMPAR blockade

(A) Mean (+ SEM) normalized synaptic sGluA1 expression in neurons (25–42 DIV) where protein synthesis was blocked with 40 μM anisomycin 30 min prior to and throughout activity blockade. For the groups left to right, n = 38, 38, 38, 34, 40, 44, 48, 48 images. Brief AMPAR blockade or brief AMPAR+AP blockade significantly (*$p < 0.05$, relative to control) enhances surface GluA1 expression at synapses in a protein synthesis-dependent manner. (B) Mean (± SEM) spontaneous syt-lum uptake from neurons (21–34 DIV) following activity blockade in the presence or absence of protein synthesis inhibitors (30 min pretreatment). For the groups left to right, n = 58, 60, 61, 60, 30, 32, 34, 32, 34, 36, 36, 36 images. Brief AMPAR blockade significantly (*$p < 0.05$, relative to control) enhances synaptic syt-lum uptake in a protein synthesis-dependent fashion. (C–D) Mean (+ SEM)

mEPSC amplitude (C) and frequency (D) in neurons (21–42 DIV) undergoing AP blockade (2 μM TTX, 3 hrs), AMPAR blockade (40 μM CNQX, 3 hrs), or AMPAR + AP blockade (3 hrs). For the indicated groups: control (n = 12, 11 cell), CNQX (n = 10, 8), TTX (n = 9, 13), TTX + CNQX (n = 10, 10). AMPAR blockade produced a significant (*$p < 0.05$, relative to control) increase in mEPSC amplitude and frequency; co-treatment with anisomycin blocked both sets of changes in mEPSCs induced by AMPAR blockade. (E) Representative examples and (F) mean (± SEM) spontaneous syt-lum uptake from neurons (24–40 DIV) following incubation with BDNF (250 ng/ml) +/− 40 μM anisomycin or 25 μM emetine (each 30 min prior to BDNF) for the indicated times. BDNF induces a time-dependent enhancement of presynaptic function (*$p < 0.05$, relative to 0 min); the same magnitude and temporal profile of BDNF-induced changes in syt uptake is observed with coincident anisomycin treatment. (G) Mean (+ SEM) syt-lum uptake induced by BDNF (250 ng/ml; 2 hr) in the presence or absence of 40 μM anisomycin or 25 μM emetine (each 30 min prior to BDNF); * $p < 0.05$ relative to non-BDNF control). (H) Representative recordings and (I) mean (+ SEM) mEPSC frequency following BDNF application (250 ng/ml; 2 hr) in the presence or absence of protein synthesis inhibitors (neurons 21–34 DIV). For the groups indicated left to right, n = 18, 11, 11, 7, 14, and 17 cells. The significant (* $p < 0.05$) increase in mEPSC frequency induced by BDNF is unaltered by protein synthesis inhibitors.

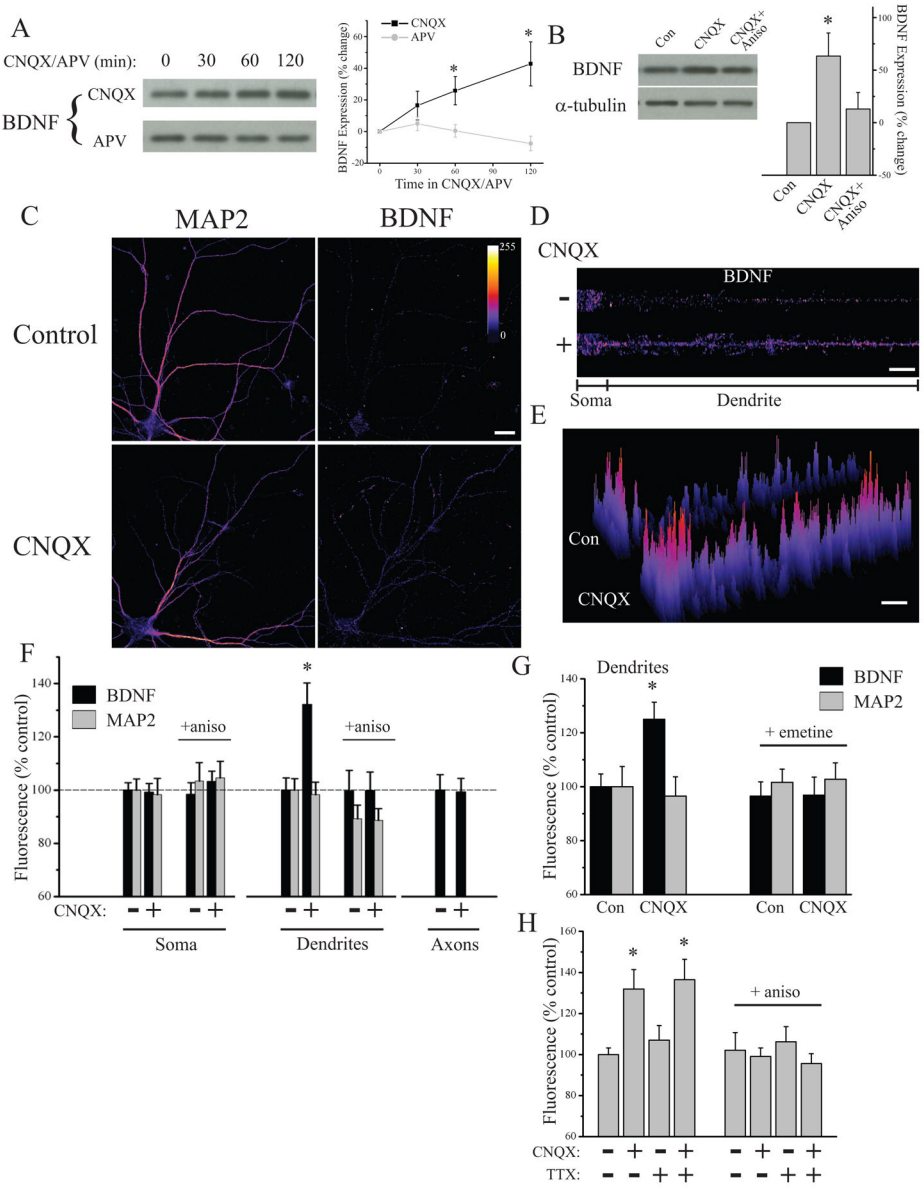

Figure 6. AMPAR blockade enhances synthesis and compartment-specific expression of BDNF

(A) Representative Western blots and summary data from experiments (21–52 DIV) examining time-dependent regulation of BDNF expression in response to 40 μM CNQX (n = 7) or 50 μM APV (n = 5); * $p < 0.05$ relative to 0 min by chi square. (B) Representative Western blots and summary data in experiments (n = 6) where neurons (DIV 21–32) were treated with CNQX (40 μM, 60 min) +/− anisomycin (40 μM, 30 min before) before harvesting; * $p < 0.05$ relative to CNQX + Aniso (t-test). (C) Representative examples of MAP2 and BDNF staining from a control neuron and one treated with CNQX (40 μM, 2 hrs). (D) BDNF expression in linearized somatic and dendritic segments from the cells shown in (C). (E) 3D plot of relative pixel intensity for the linearized images shown in (D). In (C–E), fluorescence intensity given by color-look table; Scale Bar = 20 μm. Despite similar somatic BDNF expression, dendritic BDNF expression is increased after AMPAR blockade. (F) Mean (+ SEM) expression of MAP2 and BDNF in somatic and dendritic compartments and BDNF expression in axons, normalized to average control values, in

neurons (25–36 DIV) treated as indicated. BDNF expression in dendrites was significantly (*p < 0.05, relative to control) enhanced by AMPAR blockade (n = 46) relative to control neurons (n = 47), but somatic expression from these same cells was unchanged. MAP2 expression did not differ between groups. The increase in dendritic BDNF was prevented by anisomycin (40 μM, 30 min prior to CNQX; n = 46 neurons/group). Axonal BDNF expression was unaltered by AMPAR blockade (n = 42) relative to untreated controls (n = 41). (G) Mean (+ SEM) dendritic expression of MAP2 and BDNF, normalized to the average control value, in control (untreated) neurons (n = 25) or those treated with CNQX (40 μM, 2 hrs; n = 31), CNQX + emetine (25μM, 30 min prior to CNQX; n =22), or emetine alone (n = 22). BDNF expression in dendrites was significantly (*p < 0.05, relative to control) enhanced by AMPAR blockade in a protein synthesis-dependent fashion (25–36 DIV). (H) Mean (+ SEM) normalized dendritic expression of BDNF after AMPAR blockade (40 μM CNQX, 2 hrs), AP blockade (2 μM TTX, 2 hrs), or AMPAR + AP blockade (TTX +CNQX); the same conditions were also examined with 30 min anisomycin (40 μM) pre-treatment (28–42 DIV). Alexa555-conjugated phalloidin (1:200) signal was used to identify dendrites. Both AMPAR blockade and AMPAR+AP blockade, but not AP blockade alone significantly (*p < 0.05, relative to control) enhanced dendritic BDNF expression in a protein synthesis-dependent fashion. Left to right, n = 46, 39, 39, 38, 26, 22, 20, 20 neurons.

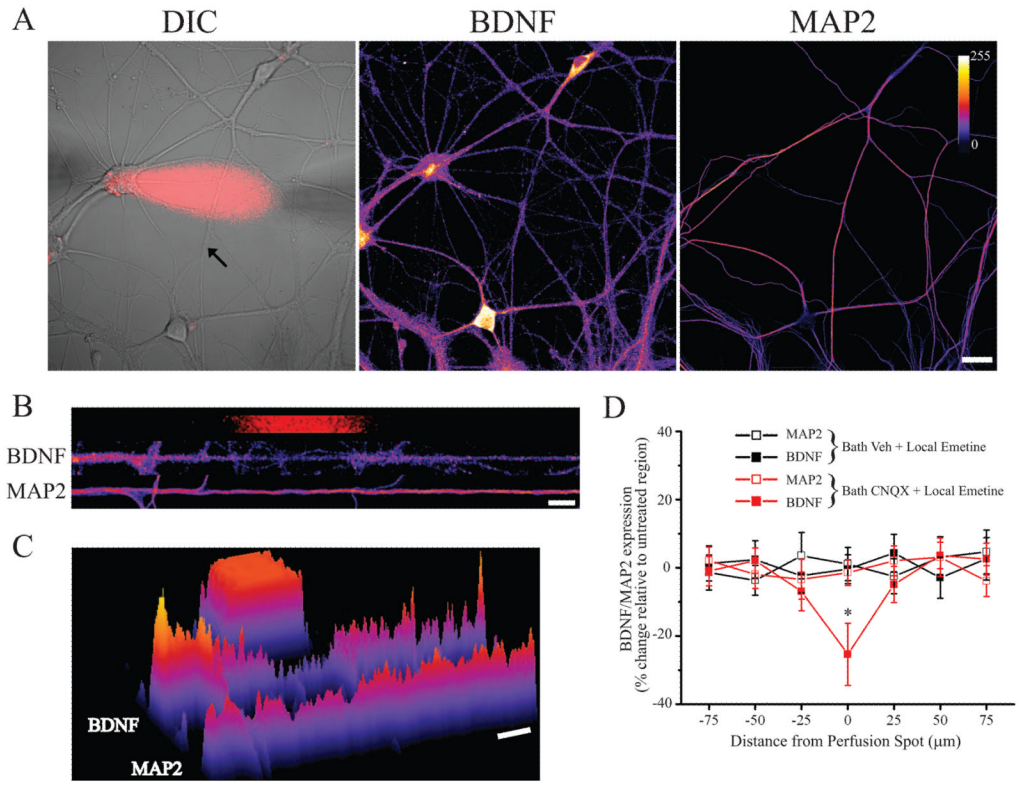

Figure 7. AMPAR blockade drives dendritic BDNF synthesis

(A) Representative DIC image of a cultured hippocampal neuron (DIV 21) with superimposed emetine (25 μM) perfusion spot (red) and the same neuron after retrospective staining for BDNF and MAP2 from an experiment including coincident AMPAR blockade (bath 40 μM CNQX, 60 min). BDNF/MAP2 fluorescence intensity indicated by color look-up table; scale bar = 20 μm. (B) Linearized dendrite indicated by the arrow cell shown in (A) with corresponding BDNF and MAP2 staining registered to the perfusion area (red). (C) 3D plot of fluorescence intensity for the dendrites shown in (B) relative to the perfusion area; a clear decrease in BDNF expression in the treated area is apparent. (D) Mean (± SEM) normalized BDNF/MAP2 expression in treated and un-treated dendritic segments from the indicated groups (21–31 DIV); all data are expressed relative to the average value in untreated segments. On the abscissa, positive and negative values indicate, respectively, segments distal and proximal from the treated area. Local emetine perfusion significantly (* $p < 0.05$) decreased BDNF expression in the treated area relative to other segments of the same dendrite when CNQX was present (n = 11 dendrites from 7 neurons), but not when vehicle was applied to the bath (n = 9 dendrites from 6 neurons); MAP2 expression in the same neurons was unaltered in the treated area.

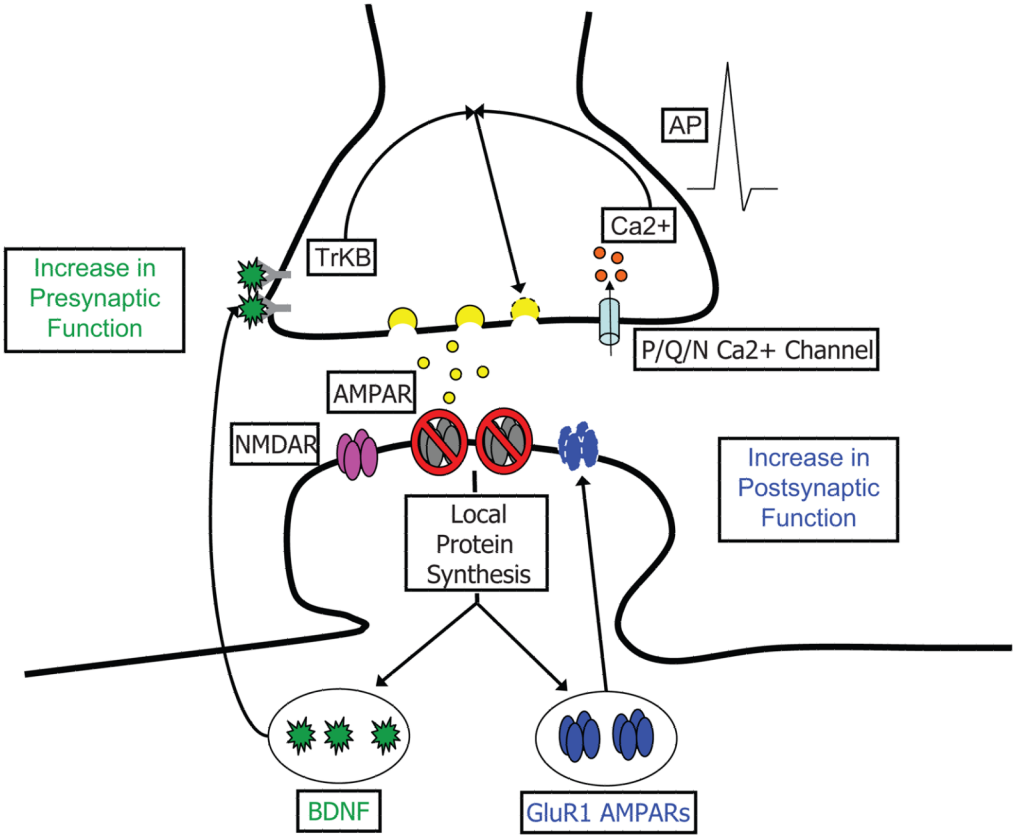

Figure 8. Parallel roles for dendritic protein synthesis in compensatory presynaptic and postsynaptic changes induced by AMPAR blockade

Model depicting key events underlying rapid homeostatic compensation. AMPAR blockade induces rapid postsynaptic compensation via synaptic incorporation of GluA1 homomeric AMPARs (Thiagarajan et al., 2005) that emerges rapidly (< 3 hrs) and requires new protein synthesis. Studies examining the effects of NMDAR mini blockade have shown that the compensatory synaptic incorporation of GluA1 homomers requires local dendritic synthesis, likely of GluA1 itself (Ju et al., 2004; Sutton et al., 2006; Aoto et al., 2008). These changes in GluA1 are observed equally in the presence and absence of spiking activity (Figure 1). In parallel, AMPAR blockade induces rapid presynaptic compensation that requires coincident activity in presynaptic terminals. The presynaptic changes require the synthesis and release of BDNF, which is locally translated in dendrites in response to AMPAR blockade.